Translation of article 10.22146/jnteti.v14i3.20175

A Machine Vision-Based Anthropometric System for Measuring Human Head Circumference

Susetyo Bagas Bhaskoro[1], Sandy Bhawana Mulia[2], Afiq Hasydhiqi[3]

[1] Cyber Physical System Study Program, Department of Manufacturing Automation Engineering and Mechatronics, Politeknik Manufaktur Bandung, Bandung, Jawa Barat 40135, Indonesia
[2] Program Studi Teknologi Rekayasa Mekatronika, Department of Manufacturing Automation Engineering and Mechatronics, Politeknik Manufaktur Bandung, Jawa Barat 40135, Indonesia
[3] Program Studi Teknologi Rekayasa Otomasi, Department of Manufacturing Automation Engineering and Mechatronics, Politeknik Manufaktur Bandung, Jawa Barat 40135, Indonesia

[Submitted: 5 March 2025, Revised: 23 May 2025, Accepted: 14 July 2025]
Corresponding Author: Susetyo Bagas Bhaskoro (email: bagas@polman-bandung.ac.id)

ABSTRACT — This study aims to develop an automated anthropometric system based on machine vision, integrated into a medical cyber-physical system (MCPS), to measure human head circumference. Head circumference is a critical parameter in growth monitoring, particularly for detecting abnormalities such as microcephaly and macrocephaly, which can affect cognitive development and overall health. To address this challenge, the study proposed an anthropometric system that enabled automated, accurate, and contactless measurements, accessible in real-time by healthcare professionals. The system was designed using a machine vision approach, incorporating object detection technology and elliptical model-based perimeter estimation to determine head circumference noninvasively. A 1,920 × 1,080-pixel (1080p) camera operating at 30 fps with a 60° field of view was mounted on a three-axis motion mechanism driven by stepper motors to automatically capture frontal and side views of the head. The measurement process began with head detection and bounding box adjustment to obtain head width parameters. Euclidean distance was used for measurement, followed by elliptical geometry modeling to estimate head circumference. Experimental results showed the lowest error rate of 2.29% at a distance of 50 cm under 300 lux lighting conditions. Performance evaluation using a confusion matrix yielded an accuracy of 92.8%, precision of 100%, recall of 97.5%, and F score of 98.7%. The proposed system provides an effective solution for healthcare professionals to perform growth screening quickly, accurately, and safely. It also supports remote healthcare services, particularly in areas with limited access to medical facilities.

KEYWORDS — Anthropometric System, Head Circumference, Noncontact Measuring Device, Machine Vision, Elliptical Perimeter, Medical Cyber-Physical System.

I. INTRODUCTION

Anthropometry is the science concerned with measuring human body dimensions and proportions. It is used to understand body size variation across populations and to detect changes that may result from environmental factors, lifestyle, or specific medical conditions [1]. Anthropometric measurements are typically performed using two main approaches: traditional and modern. Traditional methods generally rely on simple tools, such as measuring tapes, calipers, and other manual instruments. The main advantages of this approach lie in its ease of use and relatively low operational cost. However, it has notable limitations in terms of accuracy and consistency, as the results depend heavily on the skill of the examiner and are prone to subjective error.

In contrast, modern methods offer image-based approaches, including two-dimensional (2D) image and video processing techniques [2], [3]. In addition, they offer three-dimensional (3D) measurement techniques [4], [5] that provide high-precision morphological representations of the human body. These technologies, which utilize 3D scanners, photogrammetry, or sensor combinations, are capable of capturing structural details objectively and consistently, thereby improving the reliability of measurements compared to conventional methods.

With the advancement of technology, the concept of cyber-physical systems (CPS) has been extended to various sectors, including healthcare. A CPS is an integration of computing systems and physical entities via digital communication networks, enabling the development of intelligent, adaptive, and interconnected environments.

This study focuses specifically on the implementation of a medical CPS (MCPS) [6], which applies CPS principles in the medical domain. By adopting digital anthropometric technologies, human body measurements can be performed more rapidly, accurately, and efficiently. This approach is relevant to various medical applications, ranging from diagnostics to patient monitoring and rehabilitation, while also supporting the development of personalized and automated precision healthcare services.

The main focus of this study is the 2D measurement of head circumference. Head circumference serves as an important indicator for regularly monitoring individual growth and development [7]. This measurement aims to detect potential growth disorders, such as microcephaly or macrocephaly [8], which may affect cognitive development and general health. Early detection is essential to enable timely medical intervention [9]. Additionally, head size monitoring supports healthcare professionals in evaluating patient health, especially in situations where direct physical contact between doctors and patients is limited.

The measurement method proposed in this study adopts an image-based telemetry system designed to provide easy access for both patients and medical personnel. This technology enables remote measurements without requiring physical presence at healthcare facilities, making it especially beneficial for individuals with mobility limitations [10]. The system also

supports long-term monitoring with high accuracy and reduces the potential for subjective bias found in manual methods. With standardized and consistent data, medical professionals can analyze head circumference development more objectively, resulting in more precise, data-driven diagnoses.

Prior studies have investigated the application of machine vision technologies in anthropometric measurement. One study utilized digital images to measure head dimensions through image processing techniques [3]. Another used OpenPose to detect body parts such as chest, abdomen, and waist, then calculated their circumferences using elliptical perimeter formulas [1]. Research on telemetry systems has also included camera control based on human fall detection using a combination of accelerometer and gyroscope sensors [11]. These studies employed wearable devices attached directly to the body. A similar approach has been applied in bio-signal measurements through wearable devices [12], although their effectiveness remains limited by the need for direct physical contact.

Other studies explored body dimension measurements in 2D and 3D using convolutional body dimensions, point clouds, skinned multi-person linear (SMPL) models, and nonlinear regressors [13]. There are also studies on body weight estimation using body surface area derived from elliptical cylinder formulas and linear regression [14], [15], as well as object detection and waist circumference measurement using the Viola-Jones method [16]. In this study, a telemetry system combining object detection with elliptical model perimeter estimation was proposed for automated head circumference measurement. The system integrated a dual-axis movable camera with an automated height adjustment mechanism to independently identify the target object.

This study contributes to the development of automated anthropometric systems by integrating a MCPS, multi-axis moving cameras, and an object detection algorithm based on elliptical modeling to enable noncontact, real-time, and precise head circumference measurement. This approach addresses the limitations of traditional methods that rely on manual tools, such as measuring tapes or wearable devices, which require physical contact and are prone to inconsistent data [3], [11], [12]. Meanwhile, modern 3D modeling methods such as SMPL and point clouds [13] often require expensive equipment and complex setups. Wearable systems are also limited for user groups with mobility impairments or in regions with inadequate healthcare infrastructure.

The solution proposed in this study emphasizes automated, efficient, and remotely accessible measurement using a machine vision-based telemetry system. This approach offers a smart, user-friendly, and noninvasive alternative that is compatible with telemedicine platforms, thus having the potential to transform growth monitoring practices—particularly in areas with limited access to medical services. The system's advantages enable faster, safer, and more accurate screening processes. Its implications extend beyond diagnostics to include clinical evaluation, nutritional status monitoring, and even the design of head protection equipment based on valid and objective anthropometric data.

II. SYSTEM PERFORMANCE

A. OVERVIEW

Figure 1 illustrates the performance of the telemetry system for human head circumference measurement based on machine vision and MCPS technology. As shown in Figure 1, the first block diagram, representing the MCPS, includes a main subprocess responsible for data acquisition. This process begins with image capture using a camera sensor, which functions as the primary device in the measurement system. The acquired image is then analyzed to determine the centroid or geometric center of the measured object. Determining the centroid is essential, as it serves as a reference for object position stabilization, thereby improving the accuracy and consistency of the measurements [17]–[19].

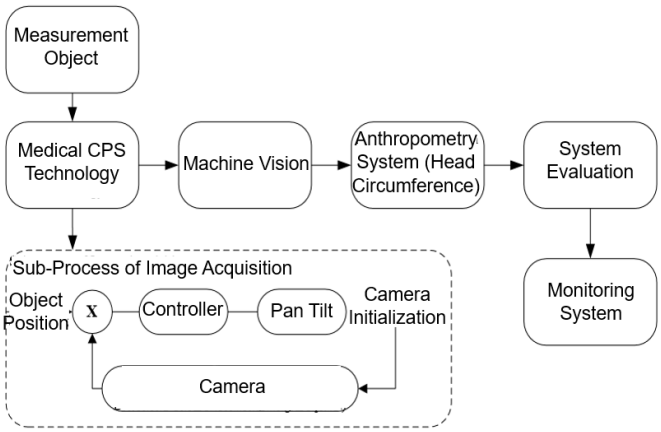

Figure 1. Performance of a machine vision-based human head circumference telemetry system.

After identifying the centroid, the system proceeds to the image identification and classification stage using machine vision. In this phase, images are analyzed based on the proportions of the human body to optimize detection and measurement accuracy [11], [12]. Machine vision plays a key role in this process as it enables automated object detection without manual interaction, thus minimizing errors caused by human factors.

In this study, the camera is integrated as the main component of the physical system within the MCPS framework. It serves as a visual sensor that captures images, which are then processed automatically by the system. The implementation of this device allows monitoring without direct contact with the measured object, which is particularly relevant in contexts requiring reduced physical interaction, such as with patients with limited mobility or during certain epidemic conditions. The integration of this technology is intended to enhance both the efficiency and accuracy of automated measurements while expanding access to telemetry-based healthcare services.

The use of the centroid in this study serves several key purposes. One of them is to determine the average position reference of the object, which assists in stabilizing and adjusting the measurement based on the object's midpoint [17]. This approach enables more accurate measurements, especially in machine vision-based monitoring processes.

This research requires consistent distance calculations, which involve converting object dimensions from pixels to millimeters. This conversion is critical, as the distance between the camera and the object must first be determined before pixel dimensions can be translated into millimeters. By identifying the centroid, the system can compute position shifts and adjust the measurement scale to achieve more precise results. Additionally, this study considers perspective correction and geometric distortion. Preliminary studies found that several

captured images exhibited perspective changes or distortions due to varying camera angles.

Therefore, a recalibration process was required to improve measurement accuracy. During the centroid determination stage, the average pixel value within a defined area was calculated using an image moment detection method. This technique enabled the computation of several image properties, such as radius, area, and center of mass, which were subsequently used to identify the centroid coordinates (x, y) of the object contour [18]. Furthermore, this study integrated a machine vision system with an object detection algorithm aimed at identifying humans and surrounding objects in an image.

The detection process is categorized into two types: soft detection and hard detection. Soft detection identifies the presence of objects without specifying their location, while hard detection not only recognizes the objects but also determines their exact position and size [20]. The study then proceeded to the anthropometric analysis stage, focusing on the measurement of various human body features.

Anthropometry in this context was categorized into two main types: static anthropometry, which pertains to measurements of body shape and composition, and dynamic anthropometry, which involves movement capability, physical strength, and spatial usage during various activities [13], [21], [22]. Table I presents the specifications of assistive tools and standard requirements used in this study to ensure the system operates optimally during the telemetry-based head circumference measurement process.

This study then continued with anthropometric analysis focusing on the measurement of human body features. During the measurement process, the object was positioned seated on a chair facing directly toward the measuring device to ensure data stability and consistency.

To obtain more accurate measurement results, the image acquisition system was designed with three distance options between the object and the camera. The closest distance used in the system was 50 cm, while the farthest distance reached 70 cm. The selection of these varying distances aimed to optimize the detection process and adjust the measurements under different lighting conditions and camera angles. This distance configuration enabled the system to analyze differences in measurement results that may arise due to perspective changes and to determine the optimal distance for the best accuracy.

Figure 2 illustrates the image acquisition stages performed by the camera. The object's position and the camera angle were arranged to comply with the predefined measurement standards. This configuration was intended to ensure optimal visual data acquisition and reduce potential distortion or errors during image analysis.

Figure 3 depicts the horizontal movement path of the camera, which was designed to move automatically from left to right. This mechanism allowed the system to adjust the camera's position to obtain the best viewing angle during the measurement process. The camera movement was only activated when the system detected the presence of an object located at the predetermined position.

Once the object was successfully identified, the system automatically captured the image. The captured image was then stored for further processing in the feature extraction and measurement stage. This extraction stage served to isolate key information from the image, such as the object's shape and

TABLE I
STANDARD SPECIFICATION REQUIREMENTS

No	Criteria	Description
1	Object measurement position	Seated position with a height between 35 - 45 cm.
2	Camera resolution	1920×1080 (1080p) / 30fps with a 60-degree field of view.
3	Light intensity	250 – 450 lux.
4	Microcontroller	NodeMCU ESP8266. input voltage: 3.3 ~ 5V. GPIO: 13 pins. PWM Channels: 10. ADC Pin: 1. Flash Memory: 4 MB. Clock Speed: 40/26/24 MHz.
5	Stepper motor	Bipolar stepper motor NEMA 17HS4401. step angle 1.8° (200 steps/rev). holding torque 40 N·cm.
6	Motor driver	A4988. Micro stepping resolution: full step. 1/2. 1/4. 1/8. and 1/16.
7	Mechanical system	Horizontal track dimensions: 1470 × 40 × 20 mm (45º angle). vertical track dimensions: 800 × 20 × 20 mm. camera mount actuator: V-slot wheel and timing belt.

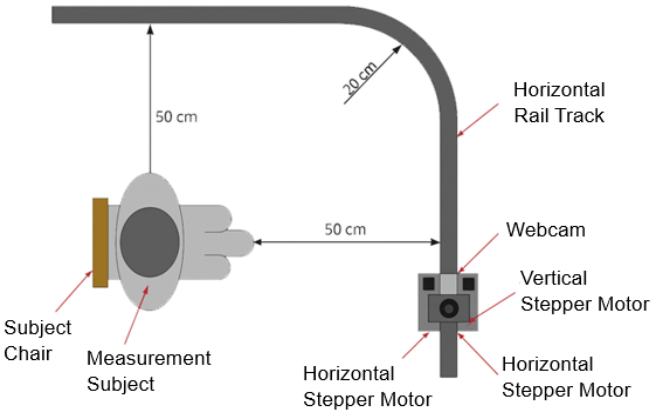

Figure 2. Camera track can move automatically.

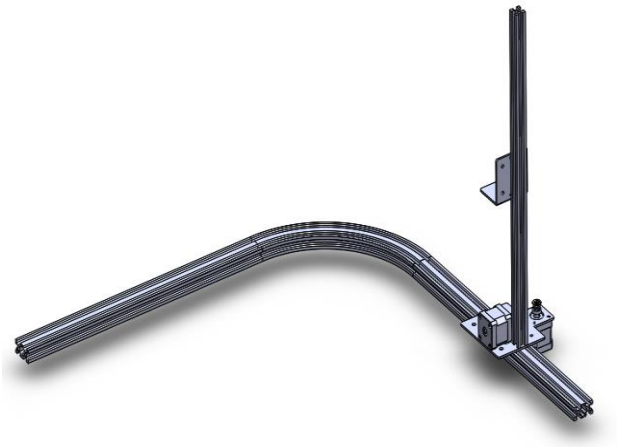

Figure 3. Camera trajectory for image capture and extraction.

dimensions, to ensure that the measurement results had a high level of accuracy [23], [24].

Through automatic horizontal movement, the system was able to optimize the image acquisition angle, resulting in more precise measurements. Moreover, this mechanism reduced human involvement in the image capture process, thereby minimizing the potential for errors caused by subjectivity or

manual mistakes. This made the system more efficient and reliable for machine vision-based measurement.

In this mechanical design, the system was equipped with a camera mount mobility track that moved along two axes using stepper motors as the primary actuators. This track was designed to allow the camera to move precisely in two directions—vertical and horizontal—to automatically adjust the viewing angle and measurement position.

The horizontal movement of the track is designed in the shape of the letter L, with the corner section formed to resemble a quarter-circle curve. This design allows the system to capture images of the object from two main viewpoints: front and side. Consequently, the system is able to obtain more comprehensive and accurate measurement data, particularly in the analysis of the shape and dimensions of the measured object.

Meanwhile, the vertical movement of the track serves to adjust the camera's height relative to the object. This mechanism is essential for enabling the system to accommodate variations in object height, ensuring that the captured image remains within the optimal field of view. With the combination of vertical and horizontal movement, the system is capable of performing detection and measurement flexibly without manual intervention, thereby improving efficiency and accuracy in machine vision-based analysis processes.

B. MEASUREMENT OF HEAD LENGTH AND WIDTH

The measurement process begins with the object detection stage. At this stage, the system is focused on identifying the frontal and side views of the head. Detection is carried out to ensure that the measured area corresponds to the predetermined parameters. Figure 4(a) shows the bounding box used to determine head length, while Figure 4(b) presents the bounding box used in measuring head width.

After the camera successfully detects and identifies the head object, the next process is the measurement of head width. This measurement is performed by adjusting the position of the bounding box so that the system can obtain accurate dimensions. At this stage, the system measures the head along the horizontal axis (x-axis), as shown in Figures 5(a) and 5(b). The data obtained from these two images are then used as the basis for further calculations.

Based on the values obtained from Figures 5(a) and 5(b), the system proceeds with the measurement process by applying the elliptical model scheme. This approach enables a more accurate estimation of head circumference because it takes into account the natural contour of the human head. The measurement result is visualized in Figure 5(c), which displays the calculated head circumference based on the elliptical model as the final output. This method yields more precise data that align with anthropometric standards used in human head growth analysis.

To determine the object's width, this study used a reference to the Euclidean distance method, which is used to measure the distance between two points in coordinate space [13], [18]. In the context of this study, the method was applied to measure the distance between coordinates along the x-axis, which was then used as the width value of the head object.

Once the width value in pixels was obtained, the measurement result was converted into centimeters (cm) to determine the actual size of the head object. The conversion process is carried out using (1).

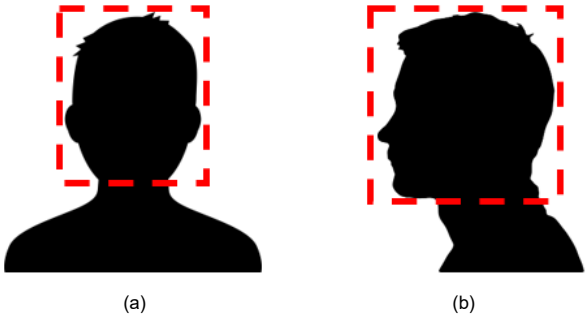

Figure 4. Head bounding box, (a) frontal view, (b) side view.

Figure 5. (a) Front-view head bounding box measurement, (b) side-view head bounding box measurement, and (c) head circumference measurement based on the elliptical model.

$$Pixel\ to\ Metric = \frac{(PixelWidth)}{(AreaWidth)}. \quad (1)$$

Equation (1) is used to calculate the ratio between the PixelWidth (width in pixels) of the object detected within the bounding box and the AreaWidth (actual width) of the measured head object. By using this ratio, the system can convert object dimensions from the digital domain (pixel-based measurement) to metric units (centimeter-based measurement), thereby producing more accurate results in accordance with anthropometric standards. This approach ensures that the head size measurements generated by the machine vision-based system achieve a high level of precision, making them suitable for various medical or anthropometric analyses related to monitoring the growth and development of the human head.

C. HEAD CIRCUMFERENCE CALCULATION

In the head circumference calculation stage, the employed approach was the elliptical perimeter formula [1], [12], [25], as shown in Figure 5(c). The measured values of the object's frontal and side view length and width were used in the calculation based on the elliptical model approximation formula, as shown in (2). In (2), a and b represent the major and minor radii of the elliptical model, respectively, estimated from the system's detection results.

$$LP \approx \pi\,[\,3(a+b) - \sqrt{(3a+b)(a+3b)}. \quad (2)$$

As a form of validation for the accuracy of the calculation using the elliptical perimeter formula, head circumference was also measured manually using a measuring tape as the conventional method. The measurement results showed that the head circumference of the object was 55 cm, with a frontal-view width of 16.4 cm (radius 8.2 cm) and a side-view width of 17.5 cm (radius 8.75 cm). The calculation using the elliptical model produced an estimated value close to the actual result,

with a difference of approximately 2 cm compared to the manual measurement. To improve the accuracy of the system, this error value was compensated through the application of pixel-to-metric conversion calibration in the measurement algorithm. This adjustment is expected to enhance the precision of the final result, thereby making the system more reliable as a supporting tool for technology-based anthropometric analysis.

D. SYSTEM TESTING FOR HEAD CIRCUMFERENCE CALCULATION

The system testing process was carried out by comparing the head circumference measurement results produced by the system with manual measurement results using a measuring tape as a reference. The purpose of this comparison was to evaluate the system's accuracy level in estimating head dimensions automatically. After all measurement data had been collected, the accuracy level was calculated by analyzing the error percentage to assess the deviation of the system results from the manual reference values.

The system's accuracy value was calculated by subtracting the measurement error from 100% [14]. In other words, the smaller the error value, the higher the system's accuracy. Equation (3) is used to calculate the error and accuracy values in the system:

$$\begin{aligned} &Error \\ &= (system\ measurement\ value \\ &- manual\ measurement\ value) \\ &/(manual\ measurement\ value) \times 100\% \end{aligned} \tag{3}$$

$$Accuracy = 100\% - accuracy$$

By applying the calculations in (3), an overview of the system's reliability in performing automatic measurements can be obtained. If the resulting accuracy value approaches 100%, the system can be considered to have good performance and can be used as an alternative for head circumference measurement through telemetry-based machine vision.

III. SYSTEM TESTING

As shown in Figure 6(a), the object to be measured was seated facing the camera mount. The positions of the camera and the object were adjusted according to a predetermined distance to ensure that the measurement could be carried out optimally. The camera automatically adjusted its position to obtain the proper view before initiating the detection and measurement process.

This study integrated a machine vision system with an object detection algorithm to detect the presence of humans and other objects in a digital image. The detection was divided into two types: soft detection and hard detection. Soft detection only identifies the existence of objects without spatial information, while hard detection is capable of determining the object's position, size, and boundary precisely [20]. To ensure that the detected head met the measurement criteria, the system automatically adjusted the camera position so that the object was located precisely at the center of the frame with an accurate frontal orientation.

The process began with the frame alignment stage, which involved an initial alignment through scanning the image area and evaluating the detection results using a bounding box. If the object was outside the optimal zone or had an incorrect orientation, the camera adjusted its position automatically via actuators until it met the predetermined standards of proportionality and orientation. Additional validation was

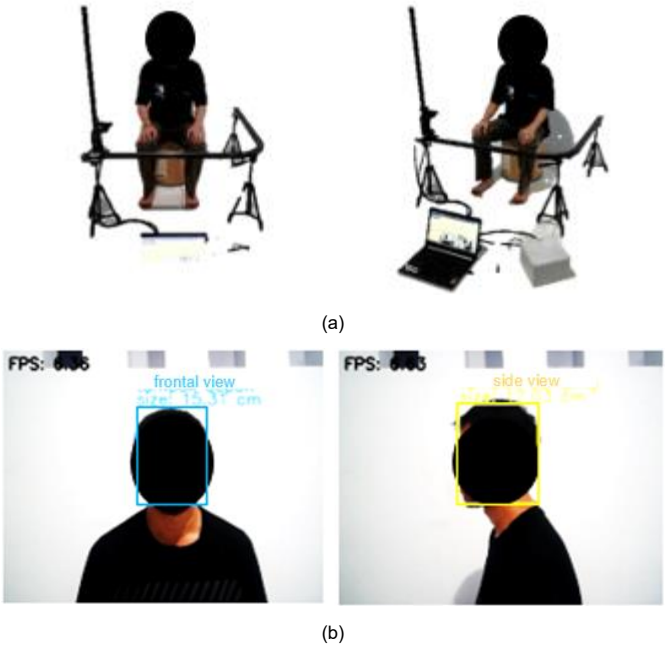

Figure 6. (a) Telemetry system implementation on a human subject, (b) bounding box implementation in the telemetry system.

conducted based on facial symmetry parameters, image clarity, and potential visual disturbances, such as the presence of dominant accessories. This approach ensured that only images with optimal quality and positioning were used in the measurement process, thereby improving the accuracy and consistency of the system in automatically detecting and computing head circumference.

After the object was successfully detected from both the frontal and side views, the system proceeded with head width measurement as the main parameter for estimating head circumference. This process is visualized in Figure 6(b), which displays the detection results used for calculating head dimensions based on the elliptical model. This approach has been proven to yield more accurate and stable measurement results compared to manual methods.

The results from the frontal and side views were then stored on the server as reference data for model training and testing. The initial dataset consisted of 420 samples and was split using an 80:20 ratio between training and testing data to ensure that the model received sufficient data for learning and was tested on unseen data.

During the testing stage, the system was evaluated based on two main categories: frontal and side views of the head. The evaluation was conducted by comparing reference annotations with the system's prediction results. System performance was analyzed using a confusion matrix, which served as the basis for calculating evaluation metrics such as accuracy, precision, recall, and F1 score to assess the effectiveness of the system in detecting and measuring head circumference automatically.

Additional testing was also performed involving human subjects wearing facial or head accessories such as glasses, masks, and hats to assess the impact of these elements on detection accuracy. As shown in Figure 7(a), this test aimed to identify potential disturbances or biases that could affect the performance of the machine vision-based measurement system.

The test results showed that the model was still able to detect human objects wearing black head coverings. This

Jurnal Nasional Teknik Elektro dan Teknologi Informasi
Volume 14 Number 3 August 2025

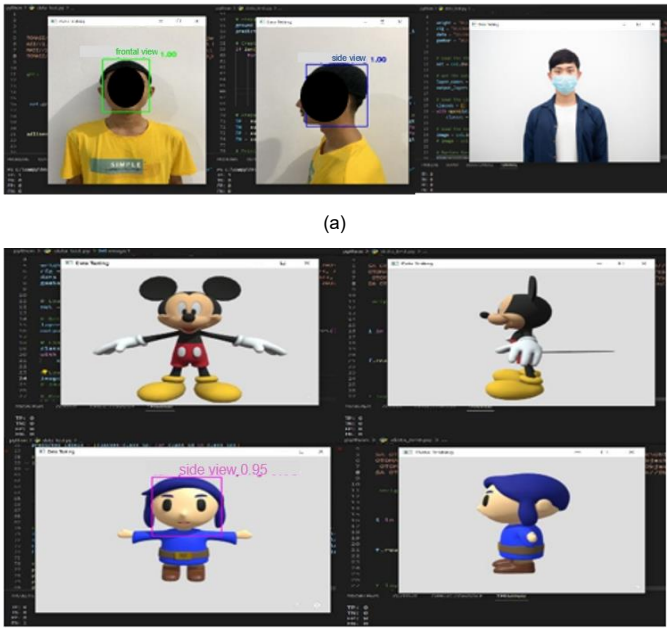

(a)

(b)

Figure 7. (a) Testing with facial accessories, (b) testing using non-human objects.

occurred because such accessories resembled hair characteristics, thus having minimal effect on the detection process. However, the model had difficulty detecting faces when the object was wearing a mask that covered a large portion of the frontal view area. This error occurred due to a mismatch between the data used in model training and the testing conditions, as the dataset used did not include facial variations with masks.

In addition to testing on human subjects, further testing was also conducted on nonhuman objects, such as animations or dolls, to evaluate the model's ability to differentiate human from non-human objects. The test results showed that the model did not produce any detection on animation or doll objects, as there were no matching annotations within the trained dataset. However, under certain conditions, false positive errors occurred, in which the model incorrectly identified nonhuman objects as humans, as shown in Figure 7(b). This error was likely caused by visual similarities between the test objects and human objects in the dataset, especially when the object had a face shape or body proportions resembling those of a human.

Based on the results of this evaluation, it can be concluded that the developed model has successfully detected human objects and distinguished between objects belonging to trained classes and those that did not. However, there remains opportunities to improve the robustness of the model, particularly in handling variations in facial accessories and reducing the likelihood of false detections involving human-like objects.

A. OBJECT DETECTION TESTING

Table II presents the results of testing several parameters that affecting the object detection process within the object detection algorithm. The tested parameters included variations in light intensity and the distance between the object and the camera. The experiments were conducted indoors using three levels of light intensity and three distance variations to evaluate the impact of these factors on system detection performance.

TABLE II
LIGHT INTENSITY PARAMETER TESTING

Lux	Object	Detection Class	Distance (cm)		
			50	60	70
300	Object without head covering	Frontal view	✓	✓	✓
		Side view	✓	✓	✓
	Object with head covering	Frontal view	✓	✓	✓
		Side view	✓	✓	✓
160	Object without head covering	Frontal view	✓	✓	✓
		Side view	✓	✓	✓
	Object with head covering	Frontal view	✓	✓	✓
		Side view	✓	✓	×
70	Object without head covering	Frontal view	✓	✓	✓
		Side view	✓	✓	✓
	Object with head covering	Frontal view	✓	✓	×
		Side view	✓	✓	×

According to the results, the object detection algorithm was able to detect objects within a light intensity range of 200–400 lux. When the light intensity was below 200 lux, the model struggled to detect objects due to insufficient contrast between the object and the background, resulting in an improperly formed bounding box. Conversely, under lighting conditions exceeding 400 lux, the model was still able to detect objects; however, excessive light reflection occasionally interfered with detection accuracy.

Furthermore, the distance between the object and the camera was also found to affect detection results. At an optimal range of 50–60 cm, detection was performed reliably. However, when the object was positioned too close (< 50 cm) or too far (> 60 cm), the model experienced a decline in accuracy due to perspective distortion, which altered the perceived size of the object in the image. These findings confirmed that both lighting intensity and object distance played a crucial role in the success of object detection, highlighting the need for proper lighting calibration and optimal distance settings to ensure maximum system performance.

B. HEAD CIRCUMFERENCE MEASUREMENT TESTING

In the head circumference measurement test, the accuracy level of the measurements produced by the designed system was evaluated, as shown in Table III. The test was conducted on six object samples, with each sample measured at three different distances to analyze the effect of distance variation on measurement accuracy. During the testing process, the lighting intensity was maintained in the range of 300–400 lux, while the distance between the object and the camera was varied to 50 cm, 60 cm, and 70 cm.

The measurements obtained from the system were then compared with manual measurements using a measuring tape, with the aim of calculating the system's accuracy and error values. Based on the results presented in Table III, the average error across all measurements at the three different distances was found to be 2.999%. Among the three distances, the 50 cm test distance yielded the best results, with an average error of 2.299%, indicating that the system provided the highest accuracy at this distance.

Several factors contributed to the measurement error values, including the distance between the object and the camera, the object's sitting posture, and the indoor lighting intensity. These factors could influence the bounding box detection and head dimension calculation; therefore, it was important to ensure

TABLE III
HEAD CIRCUMFERENCE MEASUREMENT TESTING

Distance	No.	Manual Measurement (cm)	System Measurement (cm)	Error (%)
50	1.	56	56.65	1.161
	2.	55.8	56.21	0.735
	3.	54	52.30	3.148
	4.	55	55.52	0.945
	5.	54.5	51.90	4.771
	6.	54	52.36	3.037
	Average Measurement Error			2.299
60	7.	56	51.50	8.036
	8.	55.8	54.41	2.491
	9.	54	53.30	1.296
	10.	55	53.94	1.927
	11.	54.5	52.79	3.138
	12.	54	51.80	4.074
	Average Measurement Error			3.494
70	13.	56	54.45	2.768
	14.	55.8	56.90	1.971
	15.	54	51.43	4.759
	16.	55	53.31	3.073
	17.	54.5	53.70	1.468
	18.	54	51.20	5.185
	Average Measurement Error			3.204

stable object positioning and optimal lighting conditions to enable the system to operate with maximum accuracy.

C. HEAD CIRCUMFERENCE TESTING FOR OBJECT OF DIFFERENT AGES

In addition to evaluating measurement accuracy based on distance variation, head circumference testing was also carried out according to the age differences of the objects. The purpose of this test was to ensure that the system could perform accurate measurements across various age ranges, particularly for children, since their head dimensions are smaller compared to adults. The measurement results based on the age parameter are presented in Table IV.

This test was conducted on three object samples with different age categories, namely $\leqslant$ 10 years, 12 $\leqslant$ x $\leqslant$ 23 years, and $\geqslant$ 24 years. All objects were measured at a fixed distance of 50 cm from the camera to ensure that the measurement results were not influenced by distance variation.

Based on the results in Table IV, the average measurement error is found to be 2.002%. The measurements in the $\geqslant$ 24 years category show the smallest error, at 0.179%, indicating that the system is capable of detecting head circumference with very high accuracy for adult objects. In the $\leqslant$ 10 years category, the error value is 1.569%, which remain within an acceptable range. However, in the 12 $\leqslant$ x $\leqslant$ 23 years category, the error reaches 4.259%, representing the highest among the three age groups.

These results indicate that the system achieve higher accuracy for objects with larger head sizes, such as in the 12 $\leqslant$ x $\leqslant$ 23 years and $\geqslant$ 24 years categories. A possible reason for the higher error in the teenage group is the more complex head shape variation or suboptimal lighting and object positioning during measurement. This test provides insights that the system can be further optimized to improve accuracy, particularly for objects with smaller ($\leqslant$ 10 years) or more varied head dimensions.

TABLE IV
HEAD CIRCUMFERENCE MEASUREMENT TESTING FOR OBJECTS OF DIFFERENT AGE GROUPS

Object Age (years)	Manual Measurement (cm)	System Measurement (cm)	Error (%)
$\leq$ 10	51	50.2	1.569
12 $\leq$ x $\leq$ 23	54	56.3	4.259
$\geq$ 24 yo	56	56.1	0.179
Average Measurement Error			2.002

IV. RESULTS

After several tests were conducted on the system, the results are presented in Table V, which shows the detection outcomes for the frontal and side views of the objects. The objective of this test was to evaluate the model's success rate in detecting objects with a confidence value $\geqslant$ 0.9 (highly accurate detection) and confidence < 0.9 (less accurate or poorly detected).

The test results showed that most objects were successfully detected, although some samples exhibited lower confidence values. Several factors contributed to detection errors. First, when the system was tested using non-human objects, such as dolls or animations, the model did not yield significant detection results. This indicates that the system operated according to the training dataset, which only included human objects. Second, the use of accessories—such as masks, glasses, or long hair covering the face—reduced confidence scores, as the model struggled to recognize objects when facial features were not clearly visible. Third, lighting conditions and object positioning also affected detection; suboptimal lighting or head positions inconsistent with the patterns in the training data reduced detection accuracy or caused identification failures. Based on these findings, the detailed results are presented in Table VI, which outlines the key factors influencing the system's detection accuracy.

From the results in Table VI, a performance metric was calculated to evaluate the system's effectiveness in detecting and automatically measuring head circumference. The evaluation metrics included accuracy, precision, recall, and F score.

The performance metric results are as follows. First, an accuracy of 92.8% indicated the overall correctness of the model in making accurate detections compared to the total tested samples. Precision reached 100%, showing that all detected objects truly belonged to the trained dataset class, with no false detections of non-target objects. Recall was 97.5%, meaning that most objects that should have been detected were successfully detected, although some were missed due to factors such as lighting or accessories. Finally, the F score was 98.7%, representing the harmonic mean of precision and recall, which indicated an excellent balance between detection precision and sensitivity.

From this evaluation, it can be concluded that the machine vision–based head circumference measurement system performed very well, with a low error rate. Although challenges remain in terms of lighting, object positioning, and the use of accessories, the measurement results show that the system

TABLE V
TEST RESULTS FOR FRONT AND SIDE VIEW DATASETS

Dataset Testing Results	Confidence >= 0.9	Confidence < 0.9
Frontal view	39	3
Side view	39	3

TABLE VI
CONFUSION MATRIX FROM FRONT AND SIDE VIEW DATASETS

		Annotation Class	
		Positive (1)	*Negative* (0)
Class Prediction	*Positive* (1)	TP: 74	FP: 0
	Negative (0)	FN: 2	TN: 4

TABLE VII
CONFUSION MATRIX OF THE REAL-TIME TEST DATASET FOR FRONTAL AND SIDE VIEWS OF OBJECTS

		Annotation Class	
		Positive (1)	*Negative* (0)
Prediction Class	*Positive* (1)	TP: 20	FP: 0
	Negative (0)	FN: 0	TN: 0

achieves high accuracy and can serve as a viable alternative for automatic head circumference measurement.

In real-time testing, Table VII presents the confusion matrix for frontal and side view detection. The results are as follows: the system achieve 20 true positives (TP), meaning all human objects that should have been detected as positive are correctly identified. False positives (FP) are 0, indicating no nonhuman objects are incorrectly detected as positive. False negatives (FN) are also 0, meaning no target objects go undetected. Lastly, true negatives (TN) are 0, as no negative samples are included in this test, making the TN metric irrelevant in this context.

These results indicate that the system performed exceptionally well for real-time frontal and side view object detection, as no detection errors occurred (FP = 0, FN = 0). The system achieved 100% accuracy in this scenario, demonstrating its reliability in recognizing human objects consistent with the training dataset.

V. CONCLUSION

This study concludes that the machine vision-based head circumference telemetry system, integrating an object detection algorithm and an elliptical approach for circumference calculation, is capable of automating the detection and measurement process with precision, achieving a relative error rate ranging from 2.299% to 3.494%. The system improves efficiency and consistency in anthropometric data acquisition and contributes to the development of biometric technologies that can be connected to smart devices and medical telemetry platforms. Its applications extend across multiple sectors, including public health, the wearable device industry, and real-time population monitoring. The testing results also indicate that the system can still be optimized to enhance accuracy, particularly for individuals with more extreme head dimension variations, such as children under the age of 10. Future development will focus on improving generalization across morphological diversity, validating performance under varied environmental conditions, refining system operation in dynamic contexts, and implementing adaptive mechanisms that enable automatic adjustment to object position and distance to maintain measurement consistency.

CONFLICTS OF INTEREST

The authors declare that there is no conflict of interest.

AUTHORS' CONTRIBUTIONS

Conceptualization, Susetyo Bagas Bhaskoro and Sandy Bhawana Mulia; methodology, Susetyo Bagas Bhaskoro; software, Susetyo Bagas Bhaskoro, Afiq Hasydhiqi, and Sandy Bhawana Mulia; validation, Susetyo Bagas Bhaskoro and Afiq Hasydhiqi; formal analysis, Sandy Bhawana Mulia; investigation, Sandy Bhawana Mulia and Afiq Hasydhiqi; resources, Susetyo Bagas Bhaskoro and Sandy Bhawana Mulia; data curation, Susetyo Bagas Bhaskoro and Afiq Hasydhiqi; writing—original draft, Susetyo Bagas Bhaskoro; writing—review and editing, Sandy Bhawana Mulia; visualization, Sandy Bhawana Mulia and Afiq Hasydhiqi.

REFERENCES

[1] X.Y. Gan, H. Ibrahim, and D.A. Ramli, "A simple vision based anthropometric estimation system using webcam," *J. Phys., Conf. Ser.,* vol. 1529, no. 2, pp. 1–7, Jun. 2020, doi: 10.1088/1742-6596/1529/2/022067.

[2] B.R. Lv *et al.,* "Automatic measurement of scanned human body in fixed posture," in *2010 IEEE 11th Int. Conf. Comput.-Aided Ind. Des. Concept. Des. 1*, 2010, pp. 575–578, doi: 10.1109/CAIDCD.2010.5681284.

[3] R.A. Ertürk and M.E. Karnaşak, "Anthropometric measurements with 2D images," in *Proc. 7th Int. Conf. Comput. Sci. Eng. UBMK 2022*, 2022, pp. 1–6, doi: 10.1109/UBMK55850.2022.9919504.

[4] N. Werghi, Y. Xiao, and J.P. Siebert, "A functional-based segmentation of human body scans in arbitrary postures," *IEEE Trans. Syst. Man Cybern. B (Cybern.),* vol. 36, no. 1, pp. 153–165, Feb. 2006, doi: 10.1109/TSMCB.2005.854503.

[5] P.R.M. Jones and M. Rioux, "Three-dimensional surface anthropometry: Applications to the human body," *Opt. Lasers Eng.,* vol. 28, no. 2, pp. 89–117, Sep. 1997, doi: 10.1016/S0143-8166(97)00006-7.

[6] S.J. Oks *et al.,* "Cyber-physical systems in the context of industry 4.0: A review, categorization and outlook," *Inf. Syst. Front.* vol. 26, no. 5, pp. 1731–1772, Oct. 2024, doi: 10.1007/s10796-022-10252-x.

[7] R. Shabariah, Farsida, and I. Parameswari, "Hubungan ukuran lingkar kepala dengan perkembangan anak usia 12-36 bulan berdasarkan skala denver development screening test-ii (DDST-II) di Posyandu RW 03 Mustika Jaya Bekasi Timur November 2016," *J. Kedokt. Kesehat.,* vol. 15, no. 1, Jan. 2019, doi: 10.24853/jkk.15.1.46-55.

[8] H. Sahli *et al.,* "Statistical analysis based on biometrie measures for fetal head anomaly characterization," in *2018 IEEE 4th Middle East Conf. Biomed. Eng. (MECBME),* 2018, pp. 237–242, doi: 10.1109/MECBME.2018.8402440.

[9] X. Ju *et al.,* "3D head shape analysis of suspected Zika infected infants," in *2018 11th Int. Congr. Image Signal Process. BioMed. Eng. Inform. (CISP-BMEI),* 2018, pp. 1–4, doi: 10.1109/CISP-BMEI.2018.8633125.

[10] N. Kalantari and V.G. Motti, "zCare: Designing a mobile application to support caregivers of patients with congenital Zika syndrome," in *2018 IEEE Int. Conf. Healthc. Inform. (ICHI),* 2018, pp. 276–283, doi: 10.1109/ICHI.2018.00038.

[11] R.A. Melita, S.B. Bhaskoro, and R. Subekti, "Pengendalian kamera berdasarkan deteksi posisi manusia bergerak jatuh berbasis multi sensor accelerometer dan gyroscope," *ELKOMIKA: J. Tek. Energi Elekt. Tek. Telekomun. Tek. Elektron.*, vol. 6, no. 2, pp. 259–273, May 2018, doi: 10.26760/elkomika.v6i2.259.

[12] M. Kurzyński, P. Ryba, M. Markowski, and M. Woźniak, "Medical telemetry system for monitoring and localization of patients - Functional model and algorithms for biosignals processing," *Int. J. Electron. Telecommun.*, vol. 56, no. 4, pp. 445–450, Nov. 2010, doi: 10.2478/v10177-010-0060-x.

[13] D. Škorvánková, A. Riečický, and M. Madaras, "Automatic estimation of anthropometric human body measurements," 2021, *arXiv:2112.11992.*

[14] A.B. Abadi *et al.,* "Perhitungan indeks massa tubuh less contact berbasis computer vision dan regresi linear," *Matrik: J. Manaj. Tek. Inform. Rekayasa Komput.*, vol. 21, no. 3, pp. 629–638, Jul. 2022, doi: 10.30812/matrik.v21i3.1512.

[15] C. Xiang, B. Liu, L. Zhao, and X. Zheng, "Three-dimension deep model for body mass index estimation from facial image sequences with different poses," *J. Vis. Commun. Image Represent.,* vol. 107, pp. 1–11, Mar. 2025, doi: 10.1016/j.jvcir.2024.104381.

[16] B.A. Fimaskoro, S. Aulia, and D. Rimasa, "Identification of fencing athletes based on anthropometric measurements using mediapipe pose," *J. Nas. Tek. Elekt. Teknol. Inf.*, vol. 13, no. 1, pp. 11–17, Feb. 2024, doi: 10.22146/jnteti.v13i1.8145.

[17] K. Yan *et al.,* "Face recognition based on convolution neural network," in *2017 36th Chin. Control Conf. (CCC),* 2017, pp. 4077–4081, doi: 10.23919/ChiCC.2017.8027997.

[18] B. Strbac, M. Gostovic, Z. Lukac, and D. Samardzija, "YOLO multi-camera object detection and distance estimation," in *2020 Zooming Innov. Consum. Technol. Conf. (ZINC)*, 2020, pp. 26–30, doi: 10.1109/ZINC50678.2020.9161805.

[19] A. Hazarika, A. Vyas, M. Rahmati, and Y. Wang, "Multi-camera 3D object detection for autonomous driving using deep learning and self-attention mechanism," *IEEE Access*, vol. 11, pp. 64608–64620, Jun. 2023, doi: 10.1109/ACCESS.2023.3288112.

[20] S.B. Bhaskoro, S. Aminah, and K. Taqi, "Attendance system on moving objects through face recognition using MTCNN and CNN," in *2021 3rd Int. Symp. Mater. Elect. Eng. Conf. (ISMEE),* 2021, pp. 184–189, doi: 10.1109/ISMEE54273.2021.9774257.

[21] N.-L. Dao, T. Deng, and J. Cai, "Fast and automatic body circular measurement based on a single kinect," in *Signal Inf. Process. Assoc. Annu. Summit Conf. (APSIPA),* 2014, pp. 1–4, doi: 10.1109/APSIPA.2014.7041571.

[22] M. Chao, C. Kai, and Z. Zhiwei, "Research on tobacco foreign body detection device based on machine vision," *Trans. Inst. Meas. Control,* vol. 42, no. 15, pp. 2857–2871, Nov. 2020, doi: 10.1177/0142331220929816.

[23] S.B. Bhaskoro, E.A. Salsabillah, and A.F. Rifa'i, "Sistem identifikasi manusia bergerak jatuh berdasarkan ekstraksi suara dan citra," *JTRM (J. Teknol. Rekayasa Manufaktur),* vol. 4, no. 2, pp. 101–116, Oct. 2022, doi: 10.48182/jtrm.v4i2.94.

[24] S.B. Bhaskoro, H. Supriyanto, and S. Falah, "Sistem identifikasi jumlah produk berbasis pengolahan citra dengan algoritma YOLO pada proses pengepakan industri manufaktur," *JTRM (J. Teknol. Rekayasa Manufaktur),* vol. 6, no. 1, pp. 13–28, Apr. 2024, doi: 10.48182/jtrm.v6i1.114.

[25] Y. Liu, A. Sowmya, and H. Khamis, "Single camera multi-view anthropometric measurement of human height and mid-upper arm circumference using linear regression," *PLoS One*, vol. 13, no. 4, pp. 1–22, Apr. 2018, doi: 10.1371/journal.pone.0195600.